

Cite this: *J. Mater. Chem. A*, 2019, 7, 6259

# Ultrahigh thermal conductivity of carbon allotropes with correlations with the scaled Pugh ratio†

Fancy Qian Wang,<sup>a</sup> Ming Hu <sup>\*b</sup> and Qian Wang <sup>\*a</sup>

Electrical insulators with ultrahigh thermal conductivity ( $\kappa_L$ ) are highly desirable for thermal management to facilitate heat extraction in many electronic devices. In this work, we select three typical carbon allotropes (lonsdaleite, Bct-C4, and Z-carbon) with ultrahigh  $\kappa_L$  from the 522 carbon allotropes in the Samara Database by using Boltzmann transport theory combined with first-principles calculations. We find that the thermal conductivity ( $\kappa_L$ ) of the three carbon allotropes is 1686.67, 1411.02 and 1262.05 W m<sup>-1</sup> K<sup>-1</sup>, respectively, at room temperature. A further analysis of both harmonic and anharmonic properties reveals that such high  $\kappa_L$  is attributed to their exceptional atomic structures. They all are composed of pure sp<sup>3</sup> hybridized carbon with a short bond length, small unit cell and strong chemical bonding. Together with diamond, they are the top four  $\kappa_L$  materials (beyond 1000 W m<sup>-1</sup> K<sup>-1</sup>) reported so far among the 3D carbon allotropes. Equally important, we propose a simple descriptor, namely the scaled Pugh ratio ( $G/K/n$ ), to characterize the strength of chemical bonding for high-throughput thermal material screening. The three identified carbon allotropes in this study would be alternatives to diamond in future thermal energy devices.

Received 19th December 2018

Accepted 13th February 2019

DOI: 10.1039/c8ta12236a

rsc.li/materials-a

## Introduction

Many electronic applications, such as LEDs, supercapacitors and integrated circuits, require thermal management to facilitate heat extraction, especially as the size of these devices shrinks down to the nanoscale. Therefore, searching for electrical insulators with ultrahigh lattice thermal conductivity ( $\kappa_L$ ) continues to be exciting and active in the thermal transport field.<sup>1–7</sup> Although diamond has long been recognized as an ideal candidate because of its highest thermal conductivity of 2300–3000 W m<sup>-1</sup> K<sup>-1</sup> (ref. 8–10) and a wide band gap of 5.5 eV,<sup>11</sup> it is scarce in nature and its synthetic fabrication suffers from slow growth, high cost and low quality.<sup>1</sup> Therefore, it is of intense interest to find new materials with ultrahigh thermal conductivity for efficient and safe heat spreading. However, little progress has been made since the selection criteria for ultrahigh  $\kappa_L$  of nonmetallic crystals proposed by Slack more than a decade ago.<sup>12,13</sup> The main reason is that the selection criteria are too abstract to find their corresponding physical parameters. Meanwhile, the high-throughput computation discovery of

ultrahigh  $\kappa_L$  materials is also impeded due to the lack of appropriate descriptors. Hence, it is important to fill this gap.

According to the selection criteria for ultrahigh lattice thermal conductivity  $\kappa_L$  proposed by Slack,<sup>13</sup> namely (i) a simple crystal structure, (ii) low average atomic mass, (iii) low anharmonicity, and (iv) strong interatomic bonding, we have paid close attention to the carbon-based materials with small unit cells, because they can satisfy the first two requirements. Moreover, carbon can form a large number of allotropes with sp-, sp<sup>2</sup>- and sp<sup>3</sup>-hybridizations due to its bonding flexibility,<sup>14</sup> which provides the possibility of designing new carbon-based materials. Here, we have only concentrated on the crystal structures composed of pure sp<sup>3</sup> hybridized carbon atoms as they can satisfy the criterion (iii), namely, low anharmonicity. The underlying reason is that a sp<sup>3</sup> hybridization corresponds to a tetrahedral geometry, which can make all the carbon atoms possess a tetrahedral (pyramid-shaped) arrangement, leading to a compact packing of atoms in the lattice with a high structural stiffness. Usually, such a geometrical structure can achieve low anharmonicity.<sup>15</sup> In addition, a previous study demonstrated that the bond saturation of carbon atoms, namely sp<sup>3</sup> hybridization, can significantly reduce the bond anharmonicity.<sup>16</sup> Ultimately, the key issue for achieving ultrahigh  $\kappa_L$  is to find carbon materials with strong interatomic bonding. Generally, the average bond length  $d$  is used to gauge the strength of bonding interaction in semiconductors if the harmonicity of materials is considered. However, it fails to account for the anharmonicity of lattice vibrations. Actually, there are no studies reported on any simple descriptors in estimating the anharmonicity of materials. This inhibits the progress of

<sup>a</sup>Center for Applied Physics and Technology, Department of Materials Science and Engineering, HEDPS, BKI-MEMD, College of Engineering, Peking University, Beijing 100871, China. E-mail: qianwang2@pku.edu.cn

<sup>b</sup>Department of Mechanical Engineering, University of South Carolina, Columbia, SC 29208, USA. E-mail: hu@sc.edu

† Electronic supplementary information (ESI) available: The three-phonon scattering channels of the four carbon allotropes, the elastic properties including the bulk moduli and shear moduli of all the mentioned carbon allotropes. See DOI: 10.1039/c8ta12236a

searching for materials with ultrahigh  $\kappa_L$  by using high-throughput computational methods. We note that the materials with strong chemical bonds are usually considered as brittle ones, which can withstand both the elastic and plastic deformations.<sup>17,18</sup> In such materials, highly directional bonding is desired, which can be characterized by using the Pugh ratio  $G/K$ , where  $G$  stands for the shear modulus measuring the resistance to plastic deformation, and  $K$  represents the bulk modulus calibrating the resistance to fracture.<sup>19</sup> Thus, a large Pugh ratio corresponds to strong chemical bonding, leading to weak anharmonicity of the chemical bonds. Hence, we use the Pugh ratio  $G/K$  to quantify the selection criterion (iv).

Based on the above considerations, three carbon allotropes (lonsdaleite, Bct-C4 and Z-carbon) are screened out from the 522 allotropes in the Samara Database (SACADA),<sup>20</sup> having small unit cells, short bond lengths, and large scaled Pugh ratios. The ultrahigh thermal conductivity is confirmed by systematic analysis of the phonon group velocity, three phonon phase space, three phonon scattering rates, Grüneisen parameter, atomic displacement parameters, and electron local function.

### Computational methods

The intrinsic  $\kappa_L$  is calculated by iteratively solving the linearized phonon Boltzmann transport equation (BTE)<sup>21,22</sup> with interatomic force constants derived from first-principles calculations within the framework of density functional theory (DFT) as implemented in the Vienna Ab initio Simulation Package (VASP).<sup>23</sup> Here, only the lowest order of anharmonic scattering, namely three-phonon scattering, is considered because it dominates the behavior of the thermal conductivity above and around room temperature.<sup>24,25</sup> From the solution of the BTE, the  $\kappa_L$ , as the sum of contributions over all the phonon modes  $\lambda(\mathbf{q}, j)$  with the wave vector  $\mathbf{q}$  and branch index  $j$ , can be expressed as:

$$\kappa_L^{\alpha\beta} = \frac{1}{k_B T^2 \Omega N} \sum_{\lambda} f_0(f_0 + 1) (\hbar \omega_{\lambda})^2 v_{\lambda}^{\alpha} F_{\lambda}^{\beta}, \quad (1)$$

where  $k_B$ ,  $N$  and  $\Omega$  are the Boltzmann constant, the number of uniformly spaced  $\mathbf{q}$  points in the Brillouin zone, and the volume of the unit cell, respectively.  $f_0$  is the Bose–Einstein distribution function,  $\omega_{\lambda}$  is the frequency of a phonon mode  $\lambda(\mathbf{q}, j)$ , and  $v_{\lambda}^{\alpha}$  is the component of the phonon velocity along the thermal transport direction  $\alpha$ . The  $F_{\lambda}^{\beta}$  is given by  $F_{\lambda}^{\beta} = \tau_{\lambda}^0 (v_{\lambda}^{\alpha} + \Delta_{\lambda})$ , where

$\tau_{\lambda}^0$  is the phonon lifetime of each phonon mode in relaxation time approximation (RTA) and  $\Delta_{\lambda}$  is a term used to correct the inaccuracy of RTA *via* solving the BTE iteratively. If  $\Delta_{\lambda} = 0$ , the RTA result of  $\kappa_L$  is obtained. So, the only inputs to the BTE are a series of harmonic and anharmonic interatomic force constants (IFCs), which are used to determine the phonon frequency, group velocity and lifetimes, respectively. To calculate the harmonic and anharmonic IFCs,  $5 \times 5 \times 5$ ,  $5 \times 5 \times 2$ ,  $5 \times 5 \times 3$  and  $4 \times 4 \times 4$  supercells for lonsdaleite, Bct-C4, Z-carbon, and diamond are constructed, respectively. The real-space finite displacement difference approach, which is implemented in Phonopy software<sup>26</sup> and thirdorder.py,<sup>21</sup> is applied. Based on our convergence test, the cutoff radius up to the 7<sup>th</sup>, 11<sup>th</sup>, 13<sup>th</sup>, and 17<sup>th</sup> nearest neighbors is selected to achieve converged thermal conductivities for the above four systems. In all calculations, the Perdew–Burke–Ernzerhof (PBE) for the generalized gradient approximation (GGA)<sup>27</sup> is chosen for the exchange–correlation potential, and the kinetic energy cutoff of the plane waves with a value of 520 eV is used to expand the valence electron wave functions.

## Results and discussion

### Phonon dispersion and thermal conductivity

We start with optimizing the crystal structures of lonsdaleite, Bct-C4 and Z-carbon, respectively. For comparison, the calculations for diamond are also carried out. The corresponding lattice constants are listed in Table 1, which are in good agreement with the available theoretical data.<sup>28–33</sup> The average bond length  $d$  of the four carbon allotropes is almost the same, as shown in Table 1, indicating the comparable harmonicity of their chemical bonds. We then calculate phonon dispersions of these four carbon allotropes, which determine the harmonic properties and dynamic stability of materials. As shown in Fig. 1(a)–(d), no imaginary frequencies exist in the entire Brillouin zone, confirming the dynamic stability of these allotropes. All the maximum frequencies are around 40 THz, in accordance with the fact that they have almost the same average bond length, further verifying that the three carbon allotropes studied here possess a similar bond stiffness and Debye temperature to diamond. Besides, three acoustic branches of lonsdaleite, Bct-C4 and Z-carbon are quite dispersive, which are comparable to that of diamond, indicating their large phonon group velocity ( $V_g$ ). And their average sound velocity  $V_a$  determined by elastic

**Table 1** Calculated equilibrium lattice parameters ( $a$ ,  $b$ , and  $c$ , in Å), average bond length  $d$  (in Å), Pugh ratio  $G/K$ , Grüneisen parameter  $\gamma$ , and average sound velocity  $V_a$  (in  $\text{m s}^{-1}$ ) of diamond, lonsdaleite, Bct-C4, and Z-carbon.  $n$  is the number of atoms per unit cell

	$n$	$a$	$b$	$c$	$d$	$G/K$	$\gamma$	$V_a$
Diamond	2	3.573 (3.573 (ref. 28))			1.545	1.192	0.906	13 283
Lonsdaleite	4	2.513 (2.508 (ref. 32)), (2.486 (ref. 33))		4.182 (4.183 (ref. 32)), (4.139 (ref. 33))	1.554	1.204	0.897	13 368
Bct-C4	4	4.381 (4.329 (ref. 31)), (4.38 (ref. 28))		2.512 (2.483 (ref. 31)), (2.511 (ref. 28))	1.552	1.042	1.005	12 328
Z-carbon	8	8.771 (8.771 (ref. 28)) (8.668 (ref. 29))	4.255 (4.255 (ref. 28)), (4.207 (ref. 29))	2.515 (2.514 (ref. 28)), (2.486 (ref. 29))	1.561	1.127	0.945	12 845

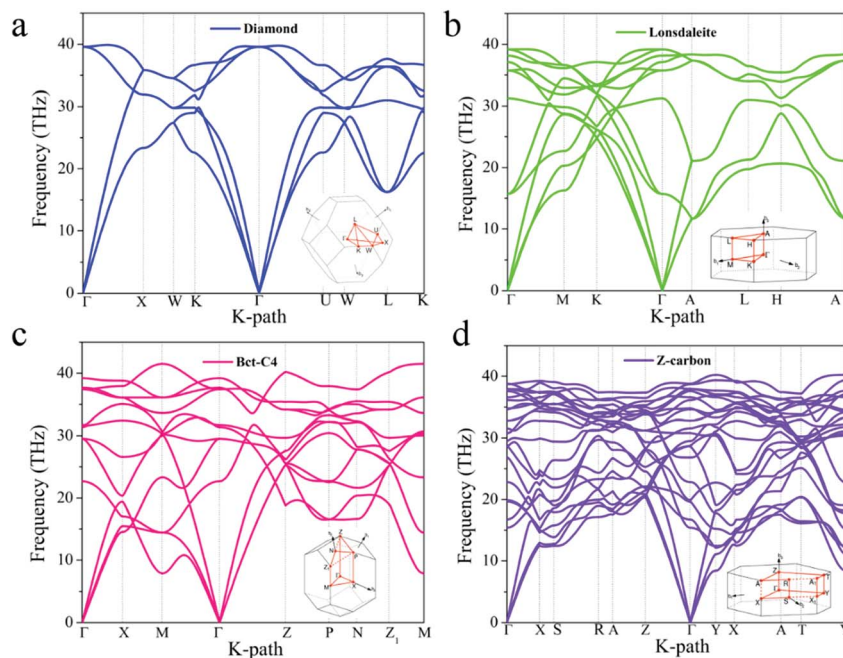


Fig. 1 Calculated phonon dispersion along the high symmetry lines for (a) diamond, (b) lonsdaleite, (c) Bct-C4, and (d) Z-carbon. The corresponding first Brillouin zones and unit cells are also shown.

properties,<sup>34</sup> as shown in Table 1, is extremely large as well as comparable, thus implying the possibility of the existence of ultrahigh thermal conductivity. As a result of the increased number of atoms per unit cell ( $n$ ), the phonon dispersions become more and more complex from diamond ( $n = 2$ ) to lonsdaleite ( $n = 4$ ) and Bct-C4 ( $n = 4$ ), and then to Z-carbon ( $n = 8$ ). Generally, a complex system with a large unit cell has a significant fraction of optical phonons that can be low-lying in energy close to the acoustic phonons.<sup>35</sup> In the three selected carbon allotropes, their optical branches with quite a large slope, are overlapped with the acoustic branches to a great extent, while in the case of diamond, the optical branches are much more localized and almost have no overlap with the three acoustic branches. Such a feature suggests that the optical phonons of lonsdaleite, Bct-C4, and Z-carbon can store a large portion of heat, and hence have non-negligible contributions to overall  $\kappa_L$  owing to their non-zero  $V_g$ . Moreover, because of the increased phonon branches, the complex system can provide much more scattering channels for three phonon scattering processes, and thus can significantly affect the  $\kappa_L$ .

We then calculate the values of thermal conductivity  $\kappa_L$  of lonsdaleite, Bct-C4, Z-carbon and diamond at room temperature (300 K) by using both the linearized BTE and relaxation time approximation (RTA). The calculated  $\kappa_L$  with contributions from the three acoustic branches (TA, TA' and LA) and all optical (OP) branches for each of them is plotted in Fig. 2. The  $\kappa_L$  of diamond is  $2303.7 \text{ W m}^{-1} \text{ K}^{-1}$ , which is in good agreement with previous studies,<sup>8,10,36</sup> showing the accuracy and reliability of our calculations. More importantly, the calculated  $\kappa_L$  of lonsdaleite, Bct-C4 and Z-carbon is 1686.67, 1411.02 and  $1262.05 \text{ W m}^{-1} \text{ K}^{-1}$ , respectively, which are much

larger than that of all the allotropes of carbon, including pure  $\text{sp}^3$  hybridized T12-carbon ( $819 \text{ W m}^{-1} \text{ K}^{-1}$ ),<sup>16</sup> T-carbon ( $33.06 \text{ W m}^{-1} \text{ K}^{-1}$ ),<sup>36</sup> pure  $\text{sp}^2$  hybridized BCO-C16 ( $444.13 \text{ W m}^{-1} \text{ K}^{-1}$ )<sup>36</sup> and 3D graphene ( $108 \text{ W m}^{-1} \text{ K}^{-1}$ ).<sup>37,38</sup> Such extremely large values indicate that, besides diamond, the three selected carbon allotropes also possess ultrahigh  $\kappa_L$  ( $>1000 \text{ W m}^{-1} \text{ K}^{-1}$ ). We note that the difference in the calculated  $\kappa_L$  obtained by RTA and iterative approaches is about 20.98%, 17.90%, 10.58%, and 8.66% for diamond, lonsdaleite, Bct-C4, and Z-carbon, respectively. In RTA, the normal (N) scattering process is wrongly treated on the same foot as the umklapp (U) scattering process, and thus the RTA only describes the umklapp process correctly.<sup>39,40</sup> So, the difference between the results of RTA and iterative approaches can describe the relative scattering strength of normal and umklapp processes. Therefore, the umklapp scattering process is predominant in the four carbon structures, and the scattering rates of the normal process are in the order of N (diamond)  $>$  N (lonsdaleite)  $>$  N (Bct-C4)  $>$  N (Z-carbon). In addition, as shown in Fig. 2, one can see the contributions of each mode to  $\kappa_L$  in these four carbon materials. In diamond, there is almost no contribution from the optical branches to the  $\kappa_L$  owing to the relatively localized optical dispersions, while the contributions from the three acoustic branches are about 45.63% (TA), 32.99% (TA'), and 20.62% (LA), respectively, which play a leading role in deciding their thermal transport. However, in the three carbon allotropes, the contributions from optical branches are comparable to those of acoustic branches. Such a difference between our selected systems and diamond is due to their quite different phonon dispersions, which is in consistent with the above discussion.

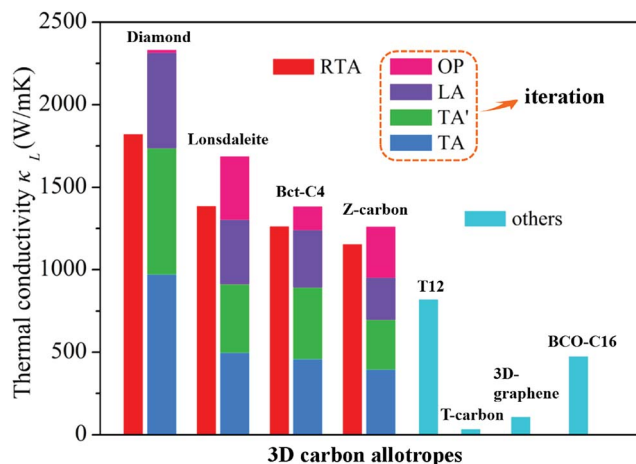


Fig. 2 Calculated lattice thermal conductivity at 300 K for the four 3D carbon allotropes using both the linearized BTE (colorful bars) and RTA (red bars). For comparison, the  $\kappa_L$  of T12, T-carbon, 3D-graphene and BCO-C16 is also given. In the iteration approach, contributions from the three acoustic branches (TA, TA' and LA) and all the optical branches (OP) to  $\kappa_L$  are marked in blue bars.

### Harmonic properties: phonon group velocity and three phonon phase space

To better understand the underlying physics governing the ultrahigh thermal conductivity in our studied carbon allotropes, the harmonic properties are analyzed including the phonon group velocity ( $V_g$ ) and three phonon phase space ( $P_3$ ). The calculated  $V_g$  with respect to frequency is plotted in Fig. 3(a).

Although the four carbon allotropes have very different geometrical structures, the variation trends of their  $V_g$  values with frequency are similar to each other with a peak at  $17.5 \text{ km s}^{-1}$ . Since  $V_g$  is proportion to  $(k/M)^{1/2}$ , where  $k$  and  $M$  denote, respectively, the force constant and mass,<sup>15,41</sup> the similar  $V_g$  with a large value in these four allotropes implies their similar strong chemical bonds, resulting in ultrahigh  $\kappa_L$ . The  $P_3$  for each of the four systems is calculated, and plotted in Fig. 3(b). The  $P_3$  is an important physical quantity used to describe how many scattering channels a material can provide, and is determined completely from the phonon dispersions of a material *via* energy and momentum conservation.<sup>42</sup> The  $P_3$  of the four materials is in the order of  $P_3$  (diamond) <  $P_3$  (lonsdaleite) <  $P_3$  (Bct-C4) <  $P_3$  (Z-carbon). Such a difference comes from the different phonon dispersions of the materials, as we discussed above. Different from diamond, the acoustic and optical branches of the three carbon allotropes are coupled with each other, which makes it much easier to satisfy the energy and momentum conservation, thus resulting in larger  $P_3$  than that of diamond. Meanwhile, we find that their thermal conductivity exactly follows the order of  $\kappa_L$  (diamond) >  $\kappa_L$  (lonsdaleite) >  $\kappa_L$  (Bct-C4) >  $\kappa_L$  (Z-carbon), verifying that an inverse relationship exists between the phase space  $P_3$  and intrinsic  $\kappa_L$  of a material.<sup>42</sup> These findings also demonstrate that the  $P_3$  should be restricted to be as small as possible in searching for materials with ultrahigh thermal conductivity.

### Anharmonic properties: three phonon scattering rates

We further study the anharmonic properties of the four carbon allotropes by calculating their three phonon scattering rates, to

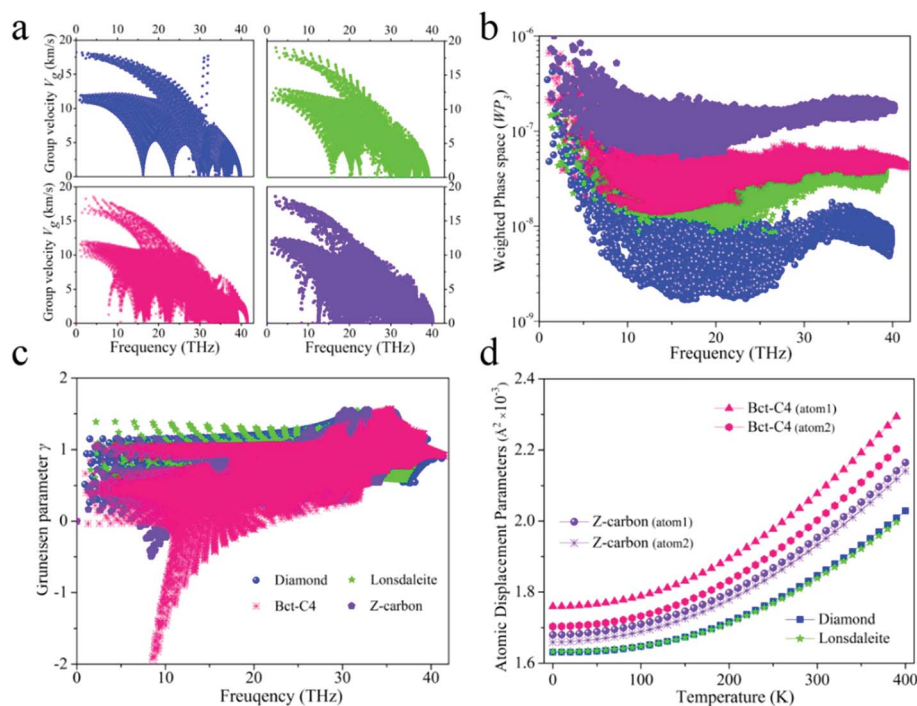


Fig. 3 Variation of (a) phonon group velocity  $V_g$ , (b) three phonon phase space  $P_3$ , and (c) Grüneisen parameter  $\gamma$  with the frequency at 300 K for diamond (dark blue), lonsdaleite (green), Bct-C4 (pink) and Z-carbon (purple), respectively. (d) Calculated atomic displacement parameters (ADPs) and the corresponding atom projections.

explore the reason why they possess the ultrahigh thermal conductivity. From the perspective of energy and momentum conservation, two types of scattering processes are involved in the three phonon scattering processes: the momentum-conserving normal (N) processes and the momentum-non-conserving umklapp (U) processes. The normal processes, which can take place with all three phonons lying within the first Brillouin zone of the corresponding lattice, merely redistribute the phonons and do not provide thermal resistance, while umklapp processes result in a thermal resistance directly. It should be mentioned that diamond possesses a unique crystal structure: all the carbon atoms are in  $sp^3$  hybridization with perfect tetrahedral arrangement with high symmetry, making the C–C bonds saturated and covalent. These features result in weak anharmonicity in diamond, leading to the highest thermal conductivity among all known bulk materials. Therefore, the anharmonicity should be kept as weak as possible in searching for candidate materials with ultrahigh thermal conductivity. On account of this, we only select the carbon allotropes composed of pure  $sp^3$  hybridized atoms, and calculate their three phonon scattering rates including both the N and U processes, simultaneously. As shown in Fig. 4(a) and (b), the calculated scattering rates have the following four features: (1) the scattering rates of N processes are much lower than those of U processes, which means that the U scattering processes are predominant in the thermal transport of those carbon materials. So, the result of RTA is close to that obtained by solving the BTE iteratively. (2) The scattering rates of optical modes are significantly higher than those of acoustic ones for the umklapp processes, which is different from the case of the normal processes. The reason is that the three-phonon scattering rates  $1/\tau$  of phonon branches generally follow a power-law dependence on frequency, namely,  $1/\tau \propto \omega^n$ ,<sup>43–45</sup> where the

exponent  $n$  for umklapp processes is always larger than that for normal processes.<sup>45–48</sup> (3) Except for diamond, the acoustic and optical branches of the three selected structures are overlapped, indicating strong coupling between the acoustic and optical branches, which is consistent with our phonon dispersion analysis. Such an overlap further confirms that the optical modes in these three structures have non-negligible contributions to the thermal conductivity. (4) The three phonon scattering rates in both U and N processes are actually comparable to each other in these four structures. Hence, our selected structures indeed preserve the weak anharmonic chemical bonds similar to that of diamond, which further confirms the validity of our selection criteria. In addition, we also specify the scattering channels of the four materials. The corresponding results can be found in Fig. S1–S3 in the ESI.†

### Anharmonicity: Grüneisen parameter, atomic displacement parameters and ELF

To quantitatively evaluate the anharmonicity of the four materials, we calculate their Grüneisen parameter  $\gamma$  and atomic displacement parameters (ADPs). Usually, a material with a soft lattice and less compact structure is likely to have a large Grüneisen parameter  $\gamma$ .<sup>15</sup> The  $\gamma$  varies with frequency as illustrated in Fig. 3(c) for the four studied systems, where the other three selected carbon allotropes indeed show a similar Grüneisen parameter  $\gamma$  to that of diamond. Besides, the averaged values of  $\gamma$ , calculated using the expression<sup>34</sup>

$$\gamma = \frac{3}{2} \left( \frac{1 + \nu}{2 - 3\nu} \right),$$

are found to be 0.906, 0.894, 1.005 and 0.945 (also shown in Table 1) for diamond, lonsdaleite, Bct-C4, and Z-carbon respectively, sharing a common feature of weak anharmonicity. Such results are in good agreement with the

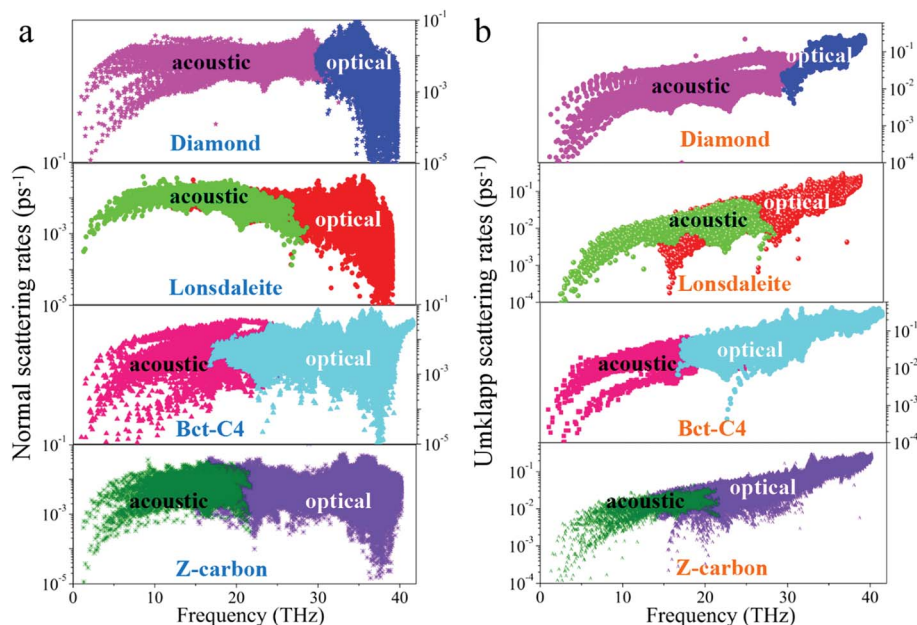


Fig. 4 Calculated three phonon scattering rates of (a) normal and (b) umklapp scattering processes for the four carbon allotropes, respectively. The contributions from the acoustic and optical branches are labeled separately.

statement that most materials in a tetrahedral local environment would have low  $\gamma$  due to their compact structures.<sup>15</sup> In addition, the atomic displacement parameter (ADP), which assesses the mean-squared displacement amplitudes of an atom around its equilibrium position in a crystal and reflects the strength of the chemical bond, is also calculated. A relatively large ADP value implies that the corresponding atom vibrates more intensively around its equilibrium position, indicating weak bonding and strong anharmonicity.<sup>49,50</sup> As shown in Fig. 3(d), the calculated ADPs of the four carbon allotropes are extremely small ( $<0.002 \text{ \AA}^2$ ), which are even one order of magnitude smaller than that of those low thermal conductivity materials, such as  $\text{SbCrSe}_3$  ( $\sim 0.03 \text{ \AA}^2$ ),<sup>51</sup>  $\text{Cu}_3\text{SbSe}_3$  ( $\sim 0.02 \text{ \AA}^2$ ),<sup>50</sup> and  $\text{CuBiS}_2$  ( $\sim 0.03 \text{ \AA}^2$ ).<sup>49</sup> The low Grüneisen parameter  $\gamma$  combined with the extremely small ADPs of the four carbon materials shows their strong chemical bonding, which is responsible for the weak anharmonicity and ultrahigh thermal conductivity of these materials.

We then calculate the electron local function (ELF) for each of the allotropes to qualitatively describe the anharmonicity of C–C bonds. The ELF has been used to characterize bonding

features in previous studies.<sup>49,52</sup> The value of the ELF ranges from 0 to 1, with 1 corresponding to the highly localized electrons and 0 corresponding to the region without electrons. To illustrate the anharmonicity, we stretch and compress the C–C bonds in the four structures, along the bond length axis by the same amount of  $0.15 \text{ \AA}$ , respectively. We only show the typical bonds of these structures in Fig. 5(a)–(f). In the harmonic model, the ELF of a bond can become fat (slim) as well as short (tall), as compared to its original state, but has no change in the shape when compressing (stretching) a bond.<sup>16</sup> From Fig. 5(a)–(f), one can see that the behaviors of the ELF of all the typical bonds are just like perfect springs, implying the low anharmonicity of all the C–C bonds.

#### Scaled Pugh ratio correlation with the thermal conductivity

As we mentioned above, the Pugh ratio  $G/K$  is a well-established parameter for justifying whether a crystalline solid is ductile or brittle, where the critical value of the  $G/K$  ratio is around  $0.57$ .<sup>19</sup> The higher the  $G/K$ , the more brittle the material. Thus, the  $G/K$  can characterize the strength of chemical bonding. The shear modulus  $G$  and bulk modulus  $K$  are calculated by using the

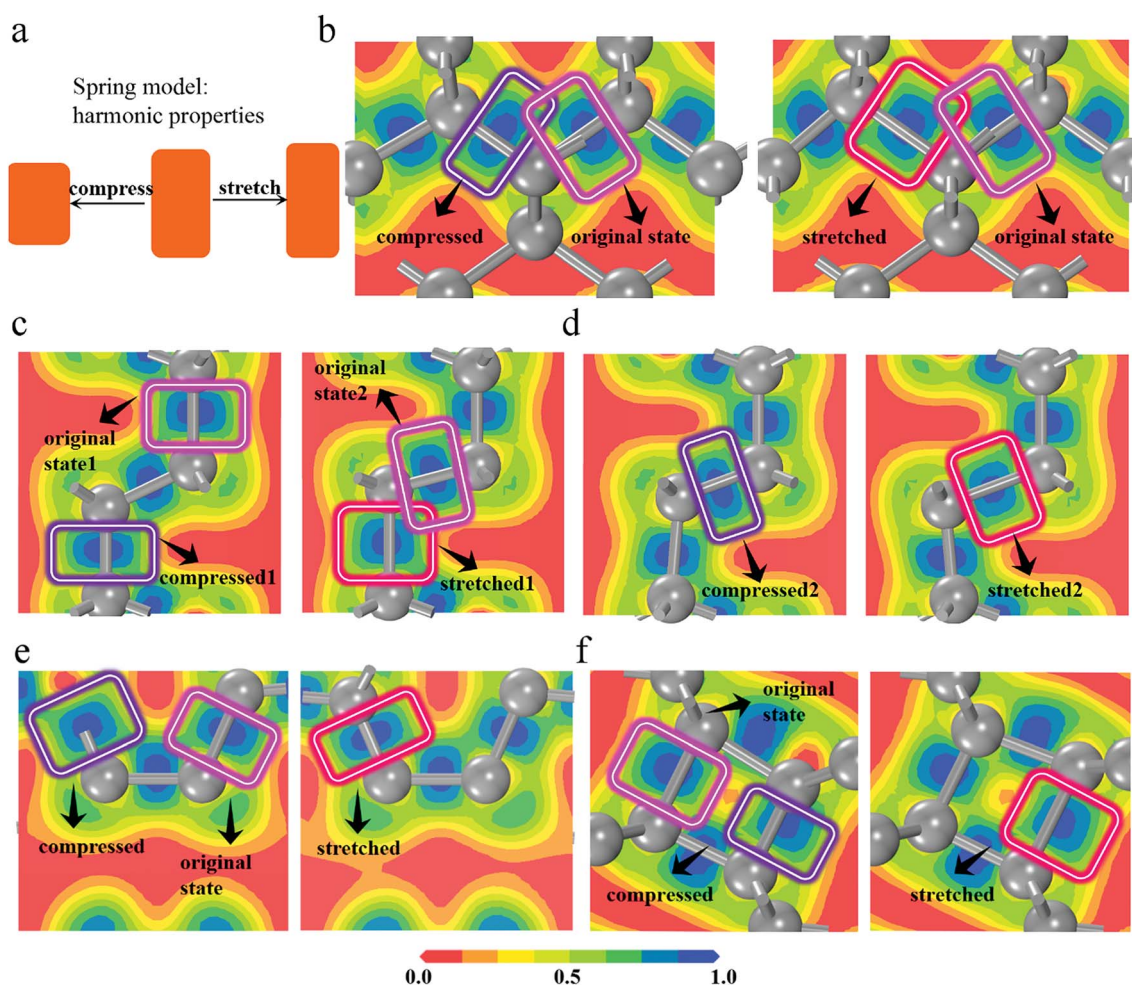


Fig. 5 (a) Spring model of the harmonic bonds. ELF contours of the typical C–C bond after being stretched (red square) and compressed (purple square) by  $0.15 \text{ \AA}$  along the bond axis for (b) diamond, (c) and (d) lonsdaleite, (e) Bct-C4, and (f) Z-carbon, respectively. The original states are highlighted in pink squares.

energy-strain method combined with the Voigt–Reuss–Hill (VRH) approximation, which is implemented in the AELAS code.<sup>19</sup> The calculated  $G/K$  of the four allotropes is displayed in Table 1, and the corresponding elastic properties can be found in ESI Table S1.† One can see that the  $G/K$  of diamond is 1.192, showing its strong bonding nature. The  $G/K$  of lonsdaleite is 1.204, slightly larger than that of diamond, while its thermal conductivity is smaller than that of diamond due to a larger number of atoms in the unit cell. As for Bct-C4, it possesses the same number of atoms as lonsdaleite, but a smaller  $G/K$  than that of lonsdaleite. So, the thermal conductivity of Bct-C4 is lower than that of lonsdaleite. In the case of Z-carbon, due to the larger unit cell it has a smaller  $\kappa_L$  as compared to that of Bct-C4. Therefore, we conclude that the thermal transport properties of carbon materials depend on both the number of atoms in the unit cell ( $n$ ) and the Pugh ratio  $G/K$ . Considering the fact that  $n$  is related to the harmonic properties of materials such as three-phonon phase space, therefore we divide the Pugh ratio by  $n$ , as scaled Pugh ratio  $G/(Kn)$ , to describe the anharmonic properties of materials. To make our results more convincing, some other carbon materials whose thermal conductivities have been calculated in previous studies,<sup>16,36–38,53</sup> are also taken into account. Besides, the  $\kappa_L$  of cubic BAs, which has been recently reported to possess ultrahigh  $\kappa_L$ ,<sup>5–7</sup> is also given only considering three-phonon scattering.<sup>1,24</sup> The  $\kappa_L$ – $G/(Kn)$  relationship is presented in Fig. 6. One can see that the  $\kappa_L$  of these carbon allotropes shows distinct correlation with their scaled Pugh ratios. The fitted curve exhibits a quadratic relationship of  $y = -6153x^2 + 7240.8x + 132.33$ , where  $y$  and  $x$  are the thermal conductivity and scaled Pugh ratio, respectively. Such a result demonstrates that the scaled  $G/(Kn)$  is indeed an appropriate descriptor for predicting the  $\kappa_L$  of carbon materials. Especially, the scaled Pugh ratio of 0.596 for diamond is the highest value, close to that of the peak point predicted from the fitted parabolic curve (0.588), corresponding to the highest  $\kappa_L$  among all 3D carbon materials. However, it should be emphasized that we

remove some of the harmonic properties of materials by dividing the number of atoms, as some previous studies did.<sup>54</sup> Thus our proposed descriptor  $G/(Kn)$  can qualitatively predict the  $\kappa_L$  of carbon allotropes. It is worth mentioning that the scaled Pugh ratio proposed in this study is based on all-carbon materials, and further studies are needed for making the extension to non-all-carbon systems.

## Conclusions

Using the state-of-the-art DFT calculations combined with solving the linearized phonon Boltzmann transport equation, we have systematically studied the intrinsic thermal transport properties of three carbon allotropes: lonsdaleite, Bct-C4, and Z-carbon. Their corresponding thermal conductivities are calculated to be 1686.67, 1411.02 and 1262.05 W m<sup>−1</sup> K<sup>−1</sup> at room temperature, respectively. Such ultrahigh thermal conductivity is attributed to their pure sp<sup>3</sup> hybridized carbon structures, small unit cell and large scaled Pugh ratio, which lead to strong chemical bonding and weak bond anharmonicity in these three allotropes. Combined with their wide band gap, the three carbon allotropes show their great potential as alternatives to diamond in future thermal energy devices.

## Conflicts of interest

The authors declare no competing financial interest.

## Acknowledgements

This work is partially supported by grants from the National Natural Science Foundation of China (Grant No. NSFC-21773004) and the National Key Research and Development Program of the Ministry of Science and Technology of China (Grants No. 2016YFE0127300 and No. 2017YFA 0205003), and is supported by the High Performance Computing Platform of Peking University, China. M. H. acknowledges the start-up fund from the University of South Carolina.

## References

- 1 L. Lindsay, D. A. Broido and T. L. Reinecke, *Phys. Rev. Lett.*, 2013, **111**, 025901.
- 2 N. Behabtu, C. C. Young, D. E. Tsentlovich, O. Kleinerman, X. Wang, A. W. K. Ma, E. A. Bengio, R. F. ter Waarbeek, J. J. de Jong, R. E. Hoogerwerf, S. B. Fairchild, J. B. Ferguson, B. Maruyama, J. Kono, Y. Talmon, Y. Cohen, M. J. Otto and M. Pasquali, *Science*, 2013, **339**, 182.
- 3 S. Berber, Y.-K. Kwon and D. Tománek, *Phys. Rev. Lett.*, 2000, **84**, 4613–4616.
- 4 M. Srikanth, Y. Keqin, L. Xuan, H. Shaoming, W. Jiangting, L. L. Hua, H. Peter, Z. Menhan, H. Jian and C. Ying, *Adv. Funct. Mater.*, 2018, **28**, 1707556.
- 5 J. S. Kang, M. Li, H. Wu, H. Nguyen and Y. Hu, *Science*, 2018, **361**, 575–578.
- 6 S. Li, Q. Zheng, Y. Lv, X. Liu, X. Wang, P. Y. Huang, D. G. Cahill and B. Lv, *Science*, 2018, **361**, 579.

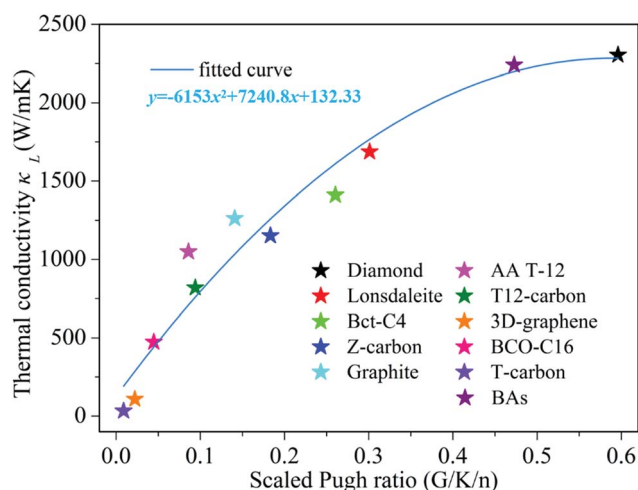


Fig. 6 Thermal conductivity of the carbon allotropes as a function of the scaled Pugh ratio ( $G/K/n$ ). For comparison, cubic BAs, which have been recently reported to possess ultrahigh  $\kappa_L$ , are also given.

- 7 F. Tian, B. Song, X. Chen, N. K. Ravichandran, Y. Lv, K. Chen, S. Sullivan, J. Kim, Y. Zhou and T.-H. Liu, *Science*, 2018, **361**, 582–585.
- 8 L. Wei, P. K. Kuo, R. L. Thomas, T. R. Anthony and W. F. Banholzer, *Phys. Rev. Lett.*, 1993, **70**, 3764–3767.
- 9 A. Ward, D. A. Broido, D. A. Stewart and G. Deinzer, *Phys. Rev. B*, 2009, **80**, 125203.
- 10 A. V. Inyushkin, A. N. Taldenkov, V. G. Ralchenko, A. P. Bolshakov, A. V. Koliadin and A. N. Katrusha, *Phys. Rev. B*, 2018, **97**, 144305.
- 11 J. Gryko, P. F. McMillan, R. F. Marzke, G. K. Ramachandran, D. Patton, S. K. Deb and O. F. Sankey, *Phys. Rev. B*, 2000, **62**, R7707.
- 12 S. L. Shindé and J. Goela, *High thermal conductivity materials*, Springer, 2006.
- 13 G. A. Slack, *J. Phys. Chem. Solids*, 1973, **34**, 321–335.
- 14 S. Zhang, J. Zhou, Q. Wang, X. Chen, Y. Kawazoe and P. Jena, *Proc. Natl. Acad. Sci. U. S. A.*, 2015, **112**, 2372.
- 15 W. G. Zeier, Z. Alex, Z. M. Gibbs, H. Geoffroy, M. G. Kanazidis and S. G. Jeffrey, *Angew. Chem., Int. Ed.*, 2016, **55**, 6826–6841.
- 16 Z. Liu, X. Wu, V. Varshney, J. Lee, G. Qin, M. Hu, A. K. Roy and T. Luo, *Nano Energy*, 2018, **45**, 1–9.
- 17 R. B. Kaner, J. J. Gilman and S. H. Tolbert, *Science*, 2005, **308**, 1268.
- 18 J. B. Levine, S. H. Tolbert and R. B. Kaner, *Adv. Funct. Mater.*, 2009, **19**, 3519–3533.
- 19 S. Zhang and R. Zhang, *Comput. Phys. Commun.*, 2017, **220**, 403–416.
- 20 H. Roald, A. A. Kabanov, A. A. Golov and D. M. Proserpio, *Angew. Chem., Int. Ed.*, 2016, **55**, 10962–10976.
- 21 W. Li, J. Carrete, N. A. Katcho and N. Mingo, *Comput. Phys. Commun.*, 2014, **185**, 1747–1758.
- 22 M. Omini and A. Sparavigna, *Physica B*, 1995, **212**, 101–112.
- 23 G. Kresse and J. Furthmüller, *Phys. Rev. B*, 1996, **54**, 11169.
- 24 D. Broido, L. Lindsay and T. Reinecke, *Phys. Rev. B*, 2013, **88**, 214303.
- 25 L. Lindsay, D. Broido and T. Reinecke, *Phys. Rev. Lett.*, 2012, **109**, 095901.
- 26 A. Togo, F. Oba and I. Tanaka, *Phys. Rev. B*, 2008, **78**, 134106.
- 27 J. P. Perdew, K. Burke and M. Ernzerhof, *Phys. Rev. Lett.*, 1996, **77**, 3865.
- 28 Z. Li, F. Gao and Z. Xu, *Phys. Rev. B*, 2012, **85**, 144115.
- 29 M. Amsler, J. A. Flores-Livas, L. Lehtovaara, F. Balima, S. A. Ghasemi, D. Machon, S. Pailhes, A. Willand, D. Caliste and S. Botti, *Phys. Rev. Lett.*, 2012, **108**, 065501.
- 30 Z. Zhao, B. Xu, X.-F. Zhou, L.-M. Wang, B. Wen, J. He, Z. Liu, H.-T. Wang and Y. Tian, *Phys. Rev. Lett.*, 2011, **107**, 215502.
- 31 K. Umemoto, R. M. Wentzcovitch, S. Saito and T. Miyake, *Phys. Rev. Lett.*, 2010, **104**, 125504.
- 32 A. Yoshiasa, Y. Murai, O. Ohtaka and T. Katsura, *J. Appl. Phys.*, 2003, **42**, 1694.
- 33 Z. Wang, F. Gao, N. Li, N. Qu, H. Gou and X. Hao, *J. Phys.: Condens. Matter*, 2009, **21**, 235401.
- 34 T. Jia, G. Chen and Y. Zhang, *Phys. Rev. B*, 2017, **95**, 155206.
- 35 C. Zhiwei, Z. Xinyue and P. Yanzhong, *Adv. Mater.*, 2018, **30**, 1705617.
- 36 S.-Y. Yue, G. Qin, X. Zhang, X. Sheng, G. Su and M. Hu, *Phys. Rev. B*, 2017, **95**, 085207.
- 37 Y. Han, J.-Y. Yang and M. Hu, *Nanoscale*, 2018, **10**, 5229–5238.
- 38 Z. Pang, X. Gu, Y. Wei, R. Yang and M. S. Dresselhaus, *Nano Lett.*, 2016, **17**, 179–185.
- 39 F. Q. Wang, J. Yu, Q. Wang, Y. Kawazoe and P. Jena, *Carbon*, 2016, **105**, 424–429.
- 40 F. Q. Wang, J. Liu, X. Li, Q. Wang and Y. Kawazoe, *Appl. Phys. Lett.*, 2017, **111**, 192102.
- 41 M. K. Jana and K. Biswas, *ACS Energy Lett.*, 2018, **3**, 1315.
- 42 L. Lindsay and D. Broido, *J. Phys.: Condens. Matter*, 2008, **20**, 165209.
- 43 L. Zhu, G. Zhang and B. Li, *Phys. Rev. B*, 2014, **90**, 214302.
- 44 L. Zhu, W. Li and F. Ding, *Nanoscale*, 2019, DOI: 10.1039/c8nr08493a.
- 45 A. Ward and D. A. Broido, *Phys. Rev. B*, 2010, **81**, 085205.
- 46 N. Mingo, *Phys. Rev. B*, 2003, **68**, 113308.
- 47 T. Luo, J. Garg, J. Shiomi, K. Esfarjani and G. Chen, *EPL*, 2013, **101**, 16001.
- 48 K. Esfarjani, G. Chen and H. T. Stokes, *Phys. Rev. B*, 2011, **84**, 085204.
- 49 Z. Feng, T. Jia, J. Zhang, Y. Wang and Y. Zhang, *Phys. Rev. B*, 2017, **96**, 235205.
- 50 W. Qiu, L. Xi, P. Wei, X. Ke, J. Yang and W. Zhang, *Proc. Natl. Acad. Sci.*, 2014, **111**, 15031–15035.
- 51 D. Yang, W. Yao, Y. Yan, W. Qiu, L. Guo, X. Lu, C. Uher, X. Han, G. Wang, T. Yang and X. Zhou, *NPG Asia Mater.*, 2017, **9**, e387.
- 52 G. Qin, Z. Qin, H. Wang and M. Hu, *Nano Energy*, 2018, **50**, 425–430.
- 53 Y. Kuang, L. Lindsay and B. Huang, *Nano Lett.*, 2015, **15**, 6121–6127.
- 54 S. Lee, K. Esfarjani, T. Luo, J. Zhou, Z. Tian and G. Chen, *Nat. Commun.*, 2014, **5**, 3525.